Supplementary Information (SI) for Nanoscale.

Non-Precious Metal High-Entropy Alloys for CO_2 Electroreduction

Runyu Xing[a,1], Xinyu Wang [a,1], Guanbo Wang[a,*], Zeyi Lu[a], Xiang Yang[a], Hongqiang Wang[b], Yun He[a], Xingyuan San[c,*], Xiaoguang Liang[a,b,d,*], Vellaisamy A. L. Roy[d]

[a]School of Physical Science and Technology, Guangxi Normal University, Guilin, 541004, P. R. China

[b]Guangxi Key Laboratory of Low Carbon Energy Materials, School of Chemical and Pharmaceutical Sciences Guangxi Normal University, Guilin, 541004, P. R. China

[c]Hebei Key Laboratory of Optic-electronic Information and Materials, The College of Physics Science and Technology, Hebei University, Baoding, 071002, China

[d]School of Science and Technology, Hong Kong Metropolitan University, Ho Man Tin, Hong Kong, P. R. China

*Corresponding authors: Guanbo Wang (1521841121@qq.com), Xingyuan San (xysan@hbu.edu.cn), and Xiaoguang Liang (lxg8521@gxnu.edu.cn)

[1]These authors contributed equally to this work.

Experimental section

Materials: Cu(II) acetylacetonate (≥97%), Co(II) acetylacetonate (≥97%), Al(III) acetylacetonate (≥98%), Fe(III) acetylacetonate (≥98%), Ni(II) acetylacetonate (≥95%), potassium bicarbonate (99.7–100.5%), ethanol (99.5%), and 1,2-hexadecanediol (98%) were purchased from Shanghai Aladdin Biochemical Technology Co., Ltd. Potassium chloride

(99.8%) and Nafion (5% in a mixture of lower aliphatic alcohols and water) were purchased from Shanghai Macklin Biochemical Technology Co., Ltd. Hydrochloric acid (HCl, 36.0–38.0%), nitric acid (HNO_3, 65.0–68.0%), and acetone (C_3H_6O, ≥99.5%) were purchased from Xilong Scientific Co., Ltd. Deuterium oxide (99.9% D, for NMR) and dimethyl sulfoxide solution (DMSO, AR, >99.8%) were purchased from Anhui Zesheng Technology Co., Ltd. Sigracet 36BB carbon paper containing micro-porous layer (MPL), cation exchange membrane (Nafion-N117), and Cu nanoparticles (30 nm) were purchased from Tianjin EVS Chemical Technology Co., Ltd. Carbon dioxide (99.999%) was purchased from Liuzhou Hengtai Gas Co., Ltd.

Preparation of CuCoAlFeNi high-entropy alloys (HEAs): CuCoAlFeNi HEA was prepared by the solvothermal method. Firstly, 5 mL of ethanol and 15 mL of acetone were transfer into a beaker (50 mL) fitted with a PTFE-coated stir bar. After stirred for 2 minutes, Cu(II) acetylacetonate (0.1 mmol), Co(II) acetylacetonate (0.1 mmol), Al(III) acetylacetonate (0.1 mmol), Fe(III) acetylacetonate (0.1 mmol), Ni(II) acetylacetonate (0.1 mmol), and 0.4 mmol of 1,2-hexadecanediol were added into the beaker. After stirring for 20 minutes, the mixture was transferred into a Teflon-lined stainless-steel autoclave, followed heating at 200 °C for 24 h. The solution was rinsed and centrifuged with ethanol. The obtained sample was dried in a vacuum oven at 60 °C for overnight.

Characterization: The morphology of CuCoAlFeNi HEA was characterized using field emission scanning electron microscopy (FESEM, Quanta 200 FEG) and transmission electron microscopy (TEM, Talos F200S). The crystalline structure and surface chemical states were analyzed by X-ray diffraction (XRD, Rigaku Mini Flex 600 with Cu Kα radiation, λ=1.54056 Å) and X-ray photoelectron spectroscopy (XPS, ThermoFisher Scientific Nexsa, Al Kα radiation). The contents of Cu, Co, Al, Fe and Ni in CuCoAlFeNi were analyzed by inductively coupled plasma optical emission spectroscopy (ICP-MS, Flexar/NexION300X). In the H-type cell, the gas products and the liquid products in cathodic electrolyte were detected by using gas chromatography (GC, PANNA A91Plus) and ^{1}H nuclear magnetic resonance (^{1}H NMR, Bruker Avance III 400 MHz), respectively. In situ Raman spectroscopy (LABRAM HR Evolution, 532 nm) was used to analyze the CO_2RR intermediates. In situ Raman spectroscopy was conducted on a commercial H-type cell at a potential of $-0.8\ V_{vs.\ RHE}$. A laser wavelength of 532 nm served as the excitation source, and the incident and scattered light were collected employing a 50x objective lens. Additionally, The H-type cell was filled with CO_2-saturated 1 M $KHCO_3$ electrolyte and connected to the electrochemical workstation, assuring that in situ experiments were conducted under the same conditions of the CO_2RR experiments.

Electrochemical CO_2 reduction measurements: Electrocatalytic CO_2RR were conducted in a conventional H-type cell and tested by an electrochemical workstation (CHI 760E, Chenhua). The H-type cell features two compartments separated by a proton exchange membrane (Nafion-N117). A standard three-electrode system was employed comprising a working electrode made of CuCoAlFeNi HEAs catalyst coated carbon paper, an Ag/AgCl reference electrode in a saturated KCl solution, and a Pt foil as the counter electrode. The carbon paper loaded with Cu nanoparticles was used as the control group. Prior to testing, the H-type cell was thoroughly cleaned by ultrasonication with 2 % nitric acid and deionized water in turn for three times. For the preparation of the working electrode, 8 mg of sample was first dispersed into a mixture of 950 μL of isopropyl alcohol and 50 μL of Nafion solution, followed by the ultrasonication for 1 h. Then, 50 μL of the mixture was dropped to the carbon paper (1×1 cm^2) and dried at room temperature for 1 h. The loading is 0.4 mg for CuCoAlFeNi HEA and Cu nanoparticles catalysts. The electrolyte in the H-type cell was 1 M of $KHCO_3$ solution. Both chambers in the H-type cell were filled with 45 mL of $KHCO_3$. Thereafter, pure CO_2 was flushed into the chambers at a flow rate of 30 sccm for 30 minutes before testing to make CO_2 saturation in $KHCO_3$ solution (pH = 8.9). The recorded applied potentials were converted to reversible hydrogen electrode (RHE) potentials by the equation as follows[1,2]:

$$E_{\text{vs. RHE}} = E_{\text{vs. Ag/AgCl}} + 0.197\ \text{V} + 0.059\times\text{pH}$$

Electrochemical properties were first performed before CO_2RR testing. The linear sweep voltammetry (LSV) curves were recorded at a scanning rate of 10 mV s^{-1}. The cyclic voltammetry (CV) scan rate was 100 mV s^{-1}. Electrochemical impedance spectroscopy (EIS) measurements were performed at a bias voltage of –0.4 V and in a frequency range from 0.1 Hz to 100 kHz. After 1000 CV cycles at a scan rate of 100 mV s^{-1}, the electrochemical active surface area (ECSA) was recorded in a non-faradaic region at scan rates of 10～200 mV s^{-1}. ECSA can be calculated according to the definition[3]:

$$ECSA = \frac{C_{dl}}{C_s}$$

The electrochemical surface area (ECSA) of as-prepared sample was estimated from their double layer capacitance (C_{dl}), which has been measured using simple cyclic voltammetry method. Where C_S is the double layer capacitance (mF cm^{-2}) of a flat surface, the specific capacitance value of C_S is 0.04 mF cm^{-2}.

CO_2RR products analysis: During the product analysis process, gaseous products analyses were quantified every 20 minutes using gas chromatography (PANNA A91Plus). The gas chromatograph was equipped with two detectors. The column was composed of capillary column and packed column. Using helium (He) and nitrogen (N_2) as double carrier gas, different gas products were analyzed. During electrolysis, the outlet end of the H-Cell was connected to gas chromatography (GC) and gas products such as H_2 and CO are detected by a thermal conductivity detector (TCD). The liquid product was tested by ^{1}H NMR with a resonance frequency of 400 MHz. 100 μL of electrolyte was mixed with 20 μL dimethyl sulfoxide and 400 μL D_2O for ^{1}H NMR testing.

The formula for calculating Faraday efficiency is as follows[4-6]:

$$\mathrm{FE_{gas}} = \frac{\mathrm{Z \times F \times v \times c}}{\mathrm{I}}$$

$$\mathrm{FE_{liquid}} = \frac{\mathrm{Z \times F \times n}}{\mathrm{Q}} = \frac{\mathrm{Z \times F \times n}}{\mathrm{I \times t}}$$

where Z is the electron transfer number, F is Faraday's constant (96485 C mol^{-1}), v is the gas flow rate at the outlet of gas chamber (L s^{-1}), c is gas concentration measured by GC (mol L^{-1}), I is the total current (A), n is the total moles of product derived from ^{1}H NMR analysis, t is reaction time (s), and Q is the total charge (C).

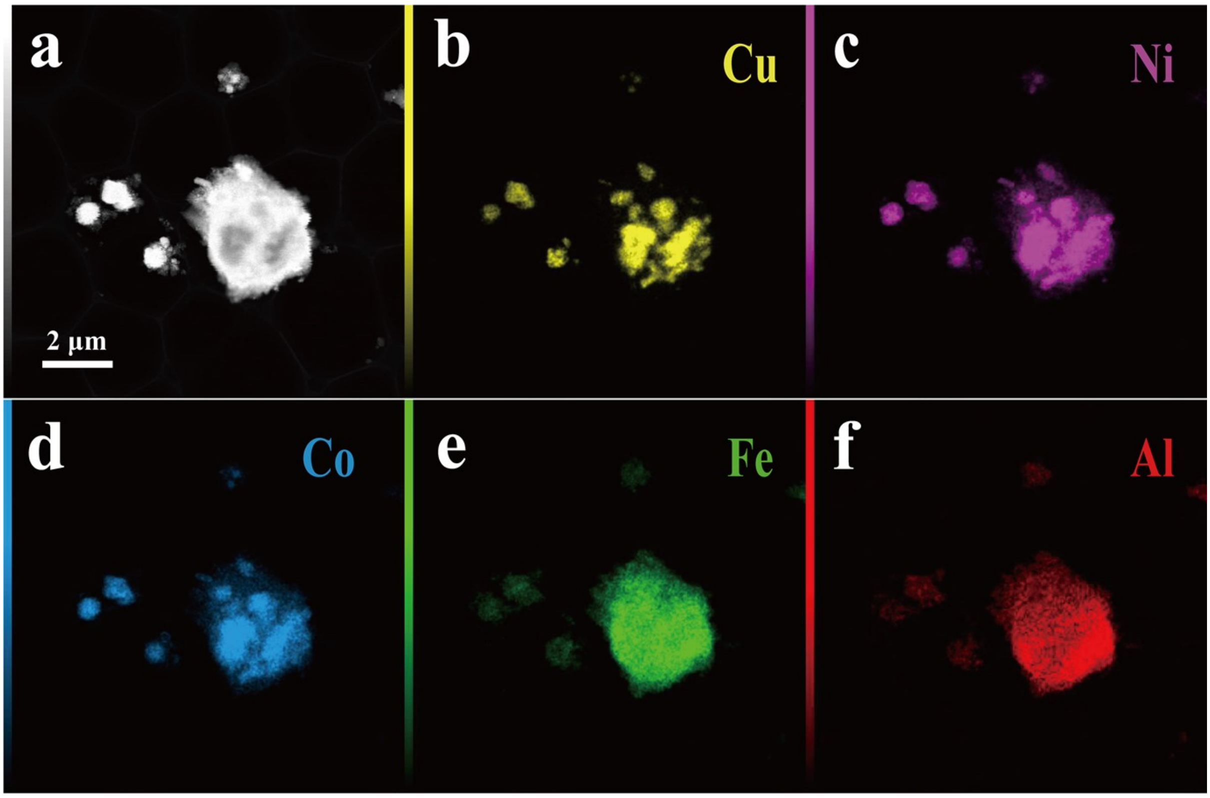

Fig. S1 Scanning TEM EDS-Mapping analysis of CuCoAlFeNi (b) Cu, (c)Ni, (d) Co, (e) Fe, and (f) Al.

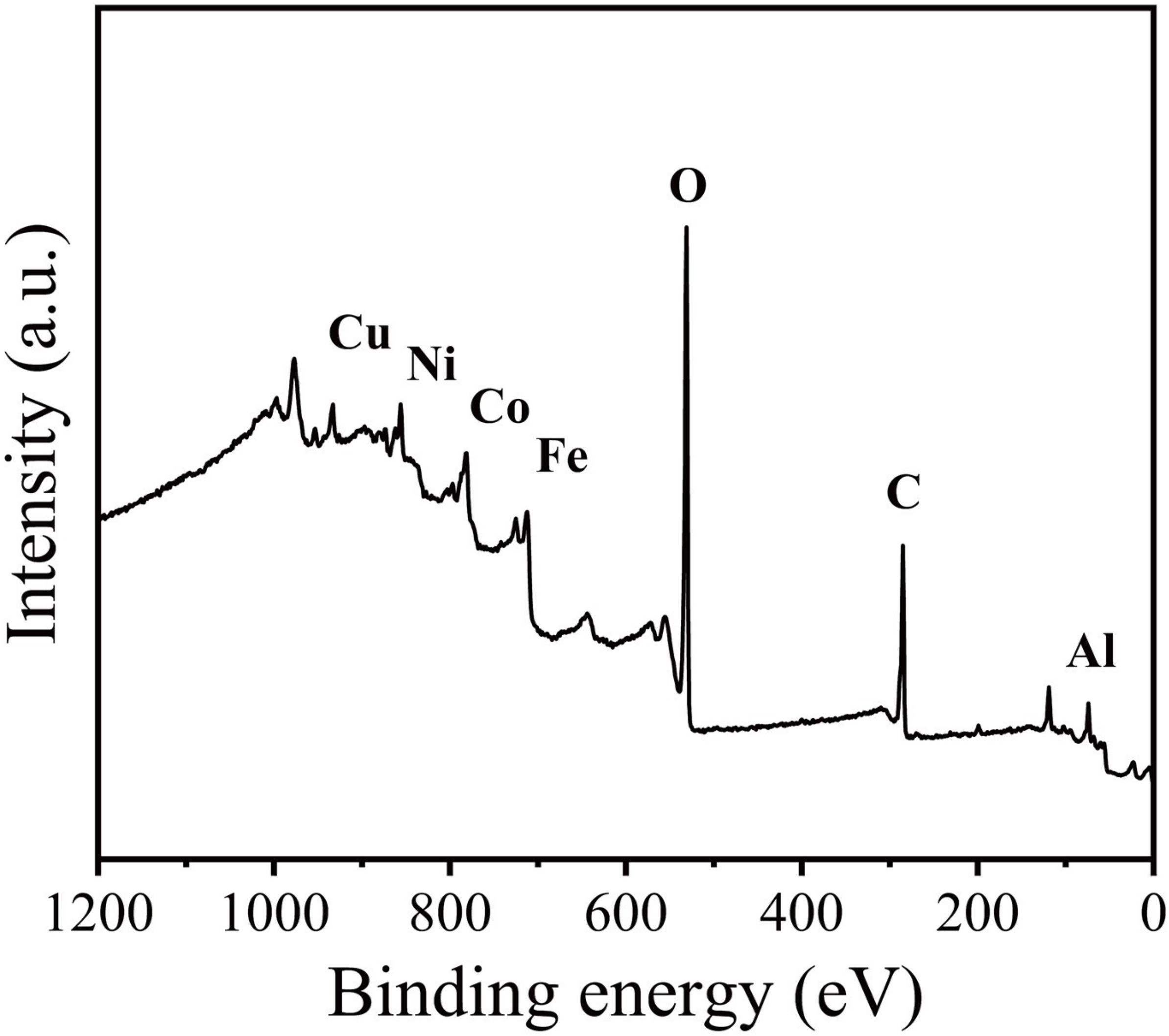

Fig. S2 Full scan XPS spectrum of CuCoAlFeNi HEA.

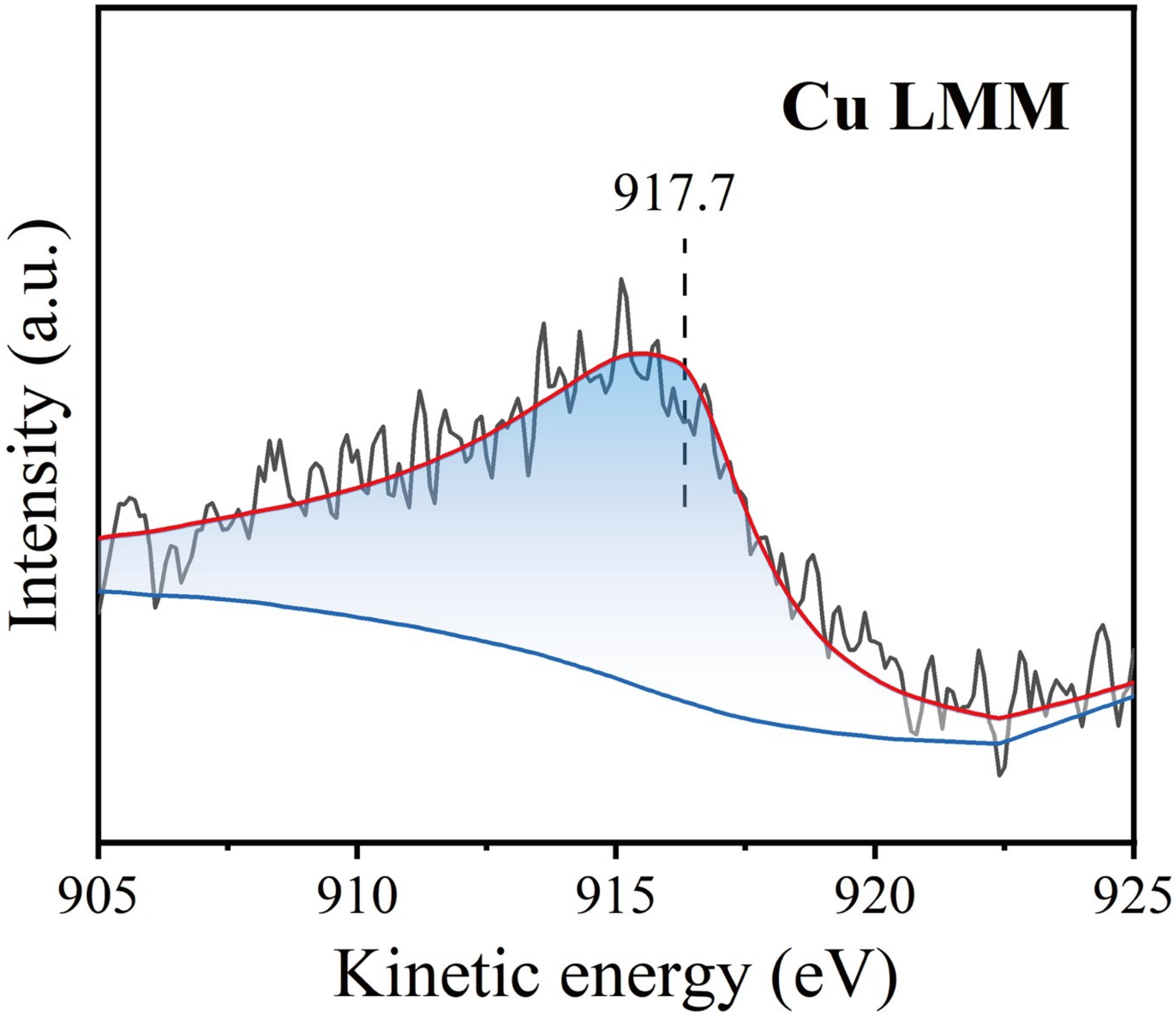

Fig. S3 Cu LMM X-ray induced Auger peaks.

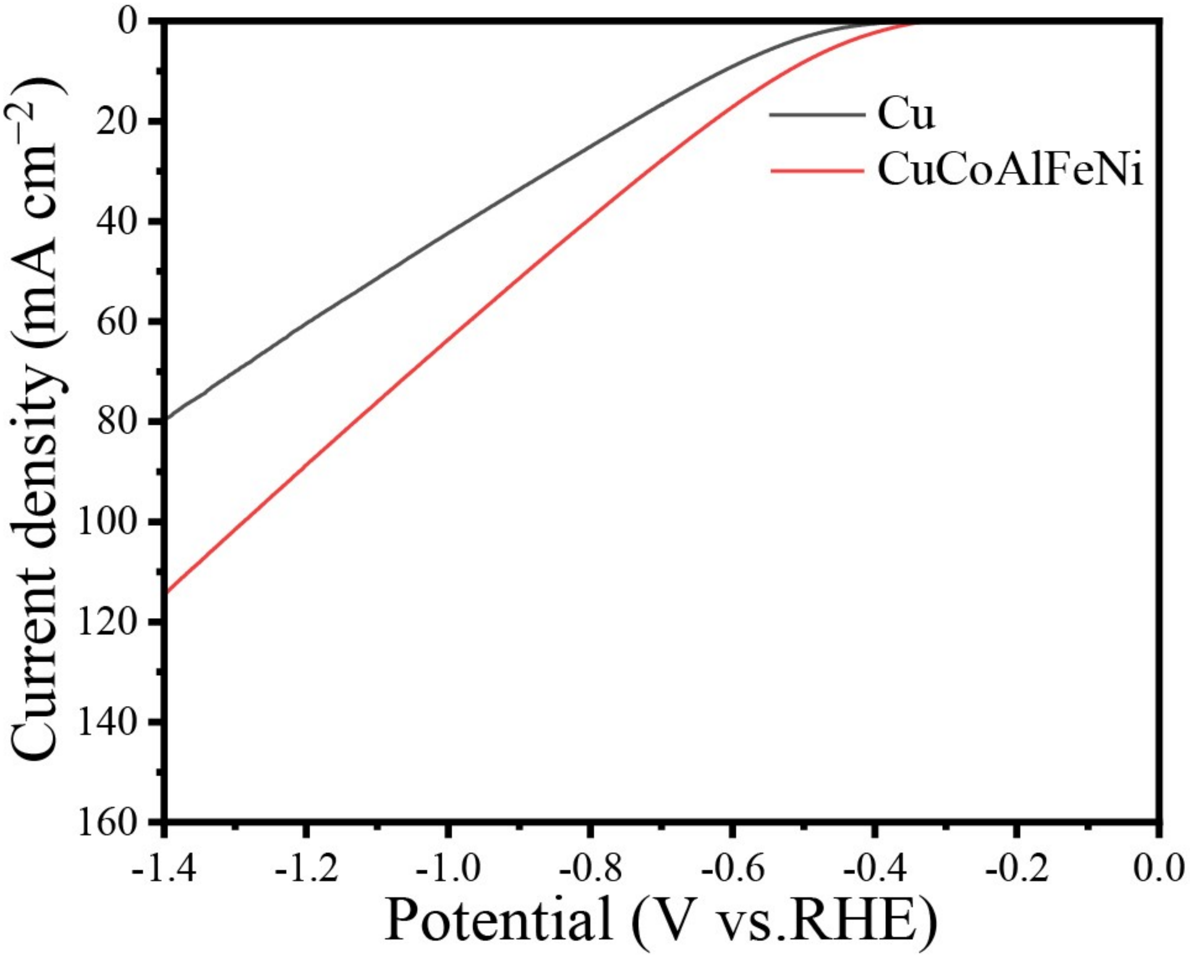

Fig. S4 The LSV profiles of Cu nanoparticles and CuCoAlFeNi HEA catalysts obtained in a N_2-saturated 1 M $KHCO_3$ solution.

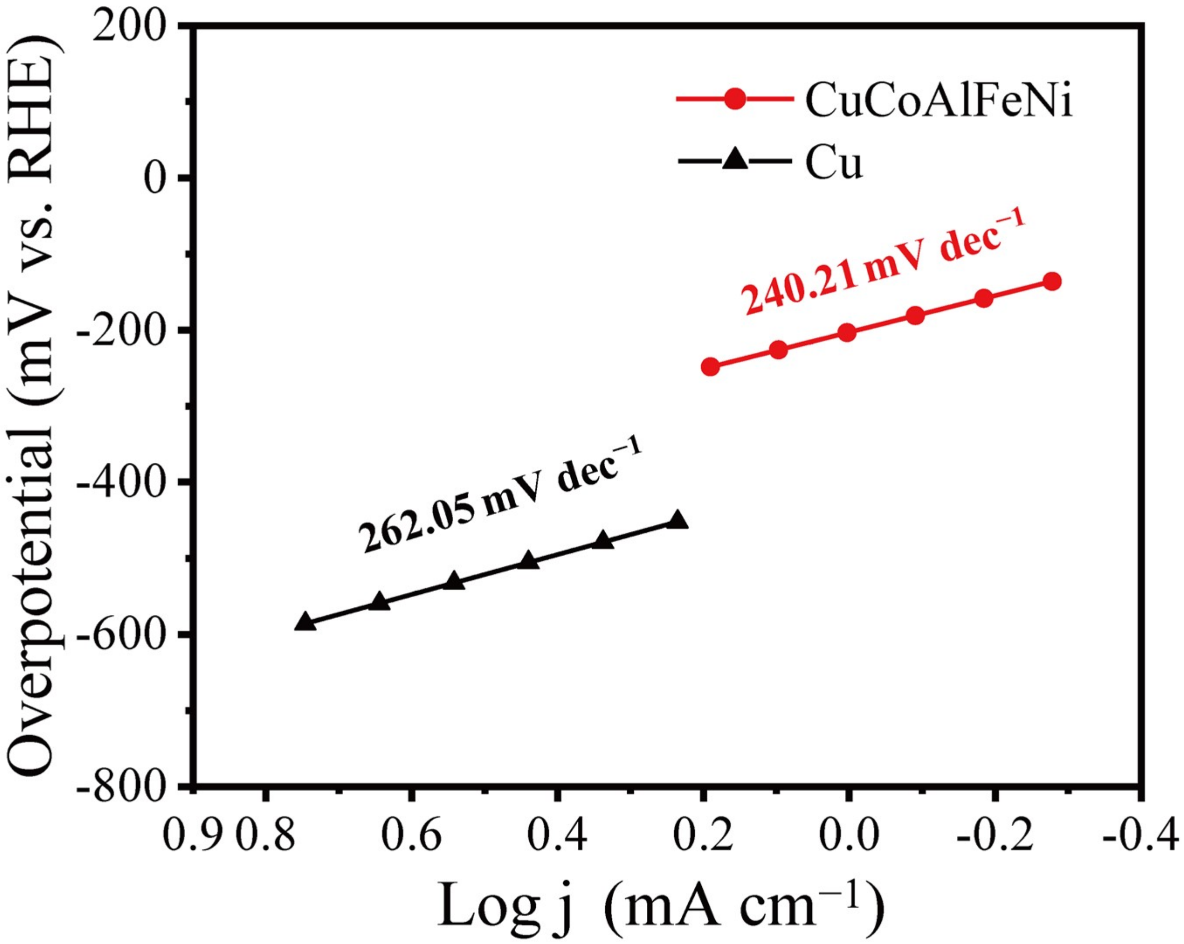

Fig. S5 Tafel plots for the electrochemical CO_2RR on the Cu nanoparticles and CuCoAlFeNi HEA tested in a 1 M $KHCO_3$ solution.

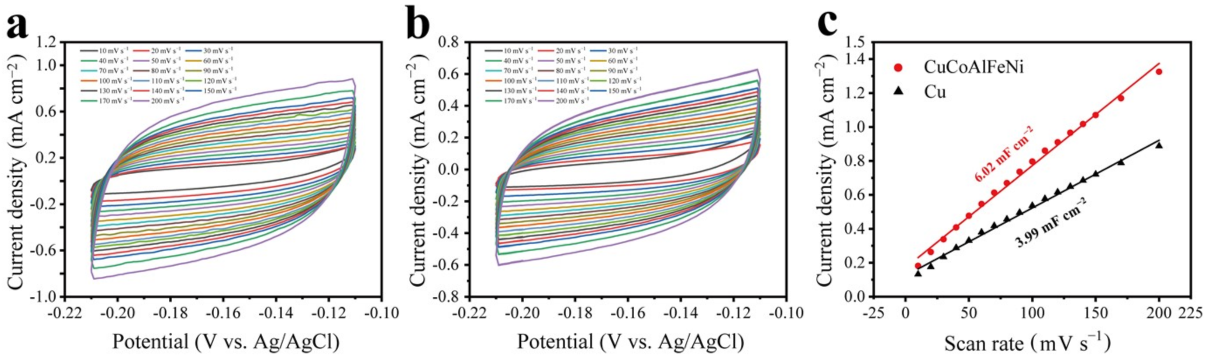

Fig. S6 CV curves of (a) CuCoAlFeNi HEA and (b) Cu tested at scan rates from 10 to 200 mV s^{-1}. (c) The corresponding current density-scan rates curves.

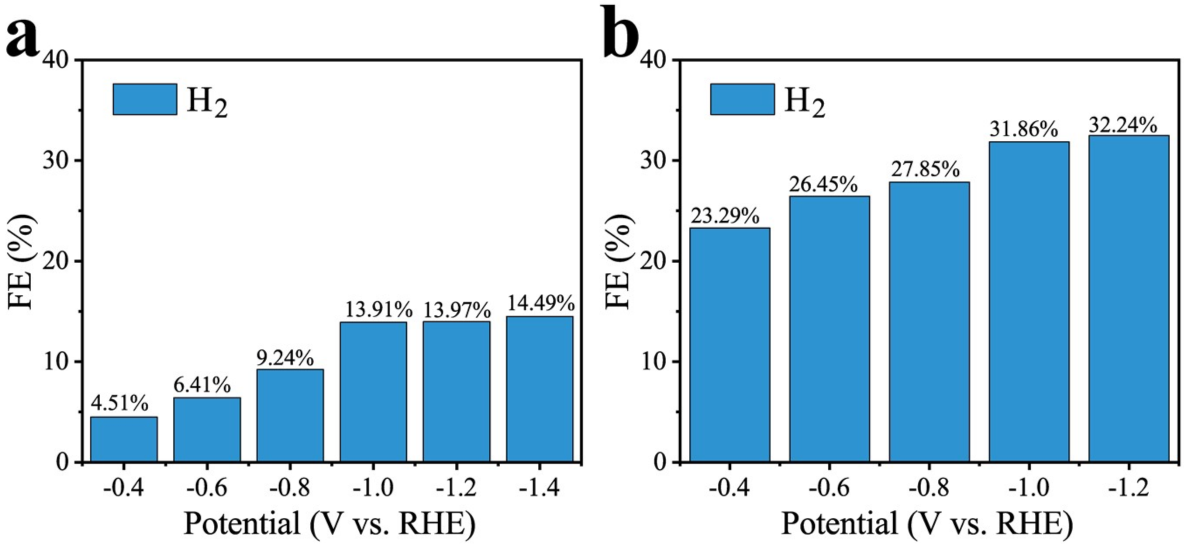

Fig. S7 The FE of CO_2RR gaseous products generated by (a) CuCoAlFeNi HEA catalysts and (b) Cu nanoparticles.

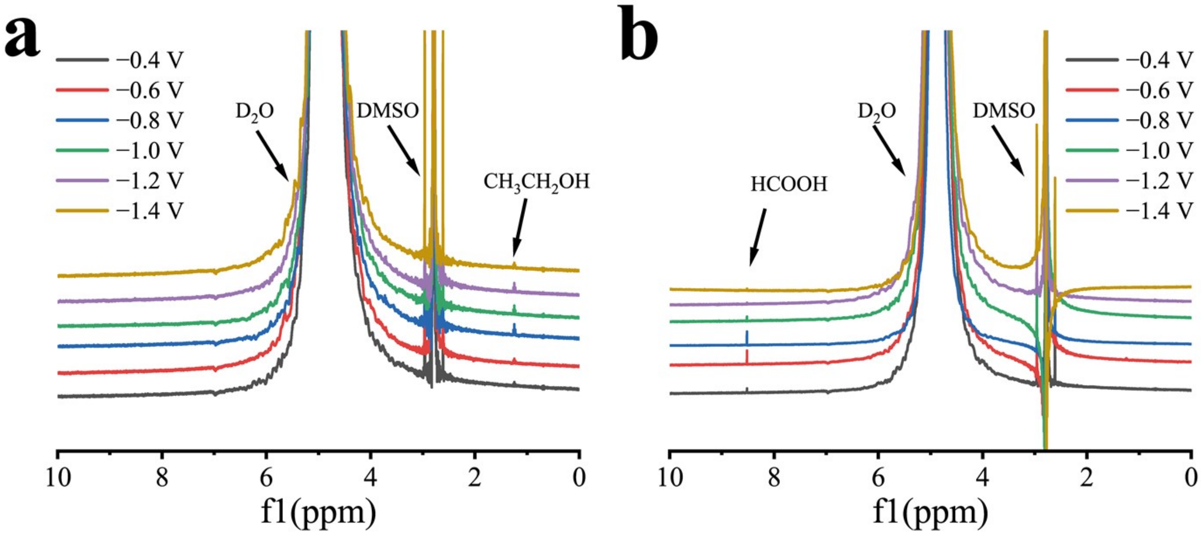

Fig. S8 The ^{1}H NMR spectra of liquid products generated by (a) CuCoAlFeNi HEA catalysts and (b) Cu nanoparticles.

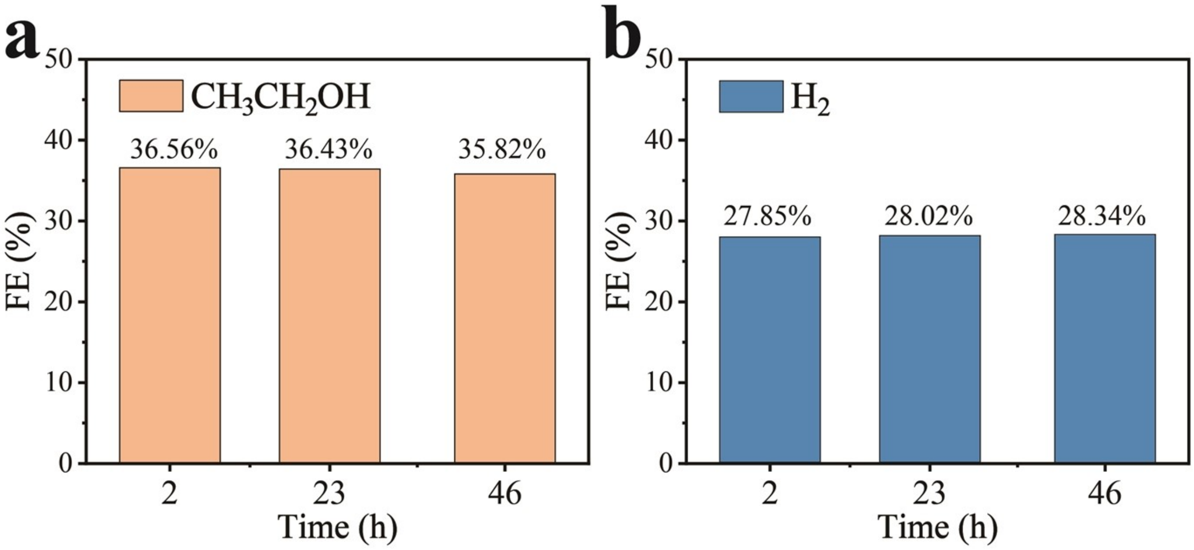

Fig. S9 The FE of (a) liquid and (b) gas products of CuCoAlFeNi HEA after stability test in an H-type cell at −0.8 V$_{\text{vs. RHE}}$ and a CO_2 flow of 10 sccm.

Table S1 The mass percentage and atomic percentage derived from inductively coupled plasma mass spectrometry in CuCoAlFeNi HEA.

	Al	Fe	Co	Ni	Cu
wt%	19.33	39.24	12.39	11.70	17.34
at%	34.04	33.43	10.01	9.51	13.01

Table S2 The values of the equivalent circuit element in the EIS impedance diagrams of Cu and CuCoAlFeNi HEAs. R_{total} represents the sum of charge-transfer impedance (R_{ct}) and electrolyte solution resistance (R_{s}).

	$R_{\mathrm{s}}(\Omega)$	$R_{\mathrm{ct}}(\Omega)$	$R_{\mathrm{total}}(\Omega)$
Cu	4.806	1.045	5.851
CuCoAlFeNi	4.362	0.669	5.031

References

1 Y. Hou, Z. Wen, S. Cui, S. Ci, S. Mao and J. Chen, Adv. Funct. Mater., 2015, 25, 872–882.

2 S. Niu, S. Li, Y. Du, X. Han and P. Xu, ACS Energy Lett., 2020, 5, 1083-1087.

3 J. Feng, C. Liu, L. Qiao, K. An, S. Lin, W. F. Ip and H. Pan, Adv. Sci., 2024, 11, 2407019.

4 Y. Zhao, L. Hao, A. Ozden, S. Liu, R.K. Miao, P. Ou, T. Alkayyali, S. Zhang, J. Ning, Y. Liang, Y. Xu, M. Fan, Y. Chen, J.E. Huang, K. Xie, J. Zhang, C.P. O'Brien, F. Li, E.H. Sargent and D. Sinton, Nat. Synth., 2023, 2, 403-412.

5 A. Ozden, Y. Wang, F. Li, M. Luo, J. Sisler, A. Thevenon, A. Rosas Hernández, T. Burdyny, Y. Lum, H. Yadegari, T. Agapie, J.C. Peters and E.H. Sargent and D. Sinton, Joule, 2021, 5, 706-719.

6 J.E. Huang, F. Li, A. Ozden, A. Sedighian Rasouli, F.P. García de Arquer, S. Liu, S. Zhang, M. Luo, X. Wang, Y. Lum, Y. Xu, K. Bertens, R.K. Miao and C.T. Dinh, Science, 2021, 372, 1074-1078.